

Improved Resolution of Thick Film Resist (Effect of Pre-Bake Condition)

Yoshihisa Sensu, Atsushi Sekiguchi
Litho Tech Japan Corporation
2-6-6 Namiki, Kawaguchi, Saitama, 332-0034, Japan
sensu@ltj.co.jp

Abstract

The effect of pre-baking conditions on the resolution and aspect ratio of thick-film resists is examined in order to improve resist processing performance. Resist samples are pre-baked at various temperatures and for various baking times, and a range of resist properties are examined. It is found that the pre-baking conditions affording the best resist pattern profile and development contrast are 125 °C for 7 min. The mechanisms responsible for the observed variations in pattern profile are studied by comparing and simulating the development activation energy, the change in the amount of solvent and photo active compound (PAC) during pre-baking, the residual solvent amount in the resist, and the transmission after pre-baking. The results indicate that there are two factors responsible for retarding the pattern formation process and causing degradation of pattern profile and resolution. One mechanism is N₂ bubbling during development, which is caused by N₂ trapped in residual solvent during exposure. The other mechanism is thermal decomposition of the PAC during baking, which weakens the retardation of development unexposed resist.

Keywords : Thick-film resist, Resolution, Pre-bake, Solvent, N₂, PAC, Benard cell, Development rate measurement system, Mask aligner, Lithography simulations

1. Introduction

Thick-film resist is used increasingly in micro-electromechanical systems (MEMS), hard disks, tape-automated bonding (TAB), bump formation on chips-on-glass (COG), chip-scale packages (CSP), and plating processes [1]. However, the thickness of such resist films precludes the direct use of thin-film resist processes for the manufacture of ICs. Reduced resolution is the major problem in processing thick-film resists, a fact that has been indicated by several researchers [2]. Therefore, thick-film resist requires photo-processes that have been specifically developed for thick films. As a continuation of the authors' previous work on optimal conditions for the development of thick-film resists [3], optimal pre-baking conditions for thick-film resist are investigated in the present study based on the effect on subsequent patterning.

When exposed, diazonaphthoquinone (DNQ) novolak-based thick-film positive resist (hereafter thick-film resist) decomposes into indene ketene, producing N₂. In a thick-film resist, the N₂ generated during the

exposure process is not released immediately from the resist film. Instead, it is released into the developer solution as development progresses, observed as N₂ bubbling. These N₂ bubbles attach to the developed resist surface, retarding the progress of development and causing problems such as reduced development activity and degraded resolution [3]. The purpose of the present research is to elucidate the mechanism of N₂ generation and bubbling during exposure of thick-film resist and to propose optimal pre-baking conditions that suppress such N₂ generation. The patterning and development properties, amount of residual solvent, refractive index, and transmission factor of the resist are examined for various pre-baking conditions, and optimal pre-baking conditions are identified.

2 Experimental Method

2.1 Overview of sample preparation

Samples were prepared at 23.5 °C and 67.0 % humidity (laboratory conditions). Fig. 1 shows the process flow employed for sample preparation. Thick-film resist (PMER P-LA900PM Tokyo Ohka Kogyo Co., Ltd., Japan) was applied to a silicon wafer to a thickness of 22 µm in a Lithotrac resist coating and baking system (Model LARC-1000 Litho Tech Japan Co., Ltd., Japan) [3]. The samples were then pre-baked by proximity baking in the Lithotech apparatus at various temperatures and various lengths of time. After baking, the samples were placed in a vacuum desiccator for 1 hr to remove water, followed by immersion in deionized water at 23.0 °C for 30 min [4]. The samples thus obtained were exposed and developed.

2.2 Pre-baking

The samples were pre-baked with a proximity gap of 0.1 mm. The pre-baking temperatures were 80, 95, 110, 125, and 140 °C, and samples were heated for 5, 7, and 9 min at each temperature. Table 1. lists the pre-baking conditions. Hereafter, the pre-baking conditions will be referred to by the baking temperature and baking time (e.g., 80-5 for 80 °C and 5 min).

2.3 Patterning

Patterning was carried out using the UL7000 mask aligner system (Quintel Corporation, USA) [3]. Exposure was performed in vacuum contact exposure mode using broadband exposure light (340 to 450 nm). The resist was then developed for 15 min using a special tetra-methyl ammonium hydroxide (TMAH) developer (PMER P-7G Tokyo Ohka Kogyo Co., Ltd.) at a controlled 23 °C in a Litho Spin Cup development system (Model SD-408 Litho Tech Japan Co., Ltd.) [3]. The resist used for evaluation was applied at a line width of 2.8 and 10.0 µm (line:space = 1:1). The exposure dose was measured using the i line wavelength (365 nm). The reference exposure dose (E_{op}) used for each pre-baking condition was the optimum dose that gives equal lines and spaces of 10.0 µm.

2.4 Evaluation

2.4.1 Pattern profile and development contrast

The developed resist pattern was observed by scanning electron microscopy (SEM; S-4000, Hitachi, Japan), and the patterning performance was evaluated based on the resolution and profile of patterns produced. In addition, for each pre-baking condition, the development contrast of the resist was measured using a resist development analyzer (RDA) [5] system at a monitoring wavelength of 950 nm. The surfaces of 10.0 μm thick films after development were observed under optical microscope.

2.4.2 Simulation

The relationship between development contrast and pattern profile was determined by inputting the measured development rate data into the SOLID-C [6] lithography simulator (SIGMA-C, Germany) and conducting simulations [7] under conditions of exposure lens NA = 0.1, coherence factor of 0.999 for the lighting system, a reduction ratio of 1:1, and best focus. The resist line width was set at 2.8 and 10.0 μm (line:space = 1:1). The exposure dose was calculated using the reference exposure dose (E_{op}) that converts a 10.0 μm wide line into 1:1 spacing for each bake conditions.

2.4.3 Activation energy

The energy of activation was evaluated based on the development rate measured for samples pre-baked at 80 to 140 °C. For each pre-baking condition employed, the energy of activation was determined by drawing an Arrhenius plot of the development rate obtained.

2.4.4 Residual solvent and photoactive compound (PAC) concentration

The change in the amount of solvent during pre-baking was measured using the PAGA-100 [8] photoacid generator analyzer (Litho Tech Japan Co., Ltd.). The PAC concentration was analyzed using the PAGA-100, the amount of residual solvent in the resist film was measured by gas chromatography mass spectrometry (GC-MS).

2.4.5 Transmission of the resist film

The transmission of the resist film was measured using the transmission measurement system (Model OOBBase32, Ocean Optics, Inc., USA). The resist-coated and pre-baked quartz substrate samples were evaluated, using a measurement wavelength of 340 to 700 nm before and after exposure at 2000 mJ/cm^2 .

3. Results

3.1 Patterning

Fig. 2 shows SEM and optical microscope of the resist patterns. Pattern resolution was deemed adequate when the thickness loss at the top was 10 % or less of the initial film thickness and the lines were clearly separated. Comparing the thickness loss at the top and the angle of the sidewall of the resist patterns for the various pre-baking conditions, the most perpendicular sidewall and least thickness loss at the top were achieved under the pre-baking condition 125-7, followed by 125-9, 110-9, 110-7, and 125-5. The thickness loss at the top was 10 % or larger for pre-baking conditions 140-5 and 140-7, which gives inadequate resolution. The highest resolution (separation resolution) was achieved for pre-baking conditions 125-7 and 125-9 (2.8 μm), followed by 110-7, 110-9, and 125-5. Under pre-baking conditions 80-7, 80-9, and 95-9, the pattern had broken and peeled off due to intensive N_2 bubbling, and pre-baking conditions 80-5, 95-5, 95-7, and 140-9 failed to provide adequate separation resolution. Traces of N_2 bubbles were observed for pre-baking conditions 80-5, 95-5, and 95-7 and large thickness loss was observed for pre-baking condition 140-9. Therefore, the most effective pre-baking condition in terms of resolution and profile of the resist pattern was found to be 125-7 followed by 125-9, 110-9, 110-7 and finally 125-5.

3.2 Results of measurements of development characteristic

Table 2. shows the measured development contrast, used as an index of resolution [9] (slope $\tan\theta$ of the dissolution rate curve) and measurements of resist sensitivity (E_{th}) for the various bake conditions. In descending order, the $\tan\theta$ measurement results were as follows: 4.3 for 125-7, 4.1 for 125-9, 3.7 for 110-9, 3.6 for 110-7, 3.5 for 125-5, 3.3 for 140-5, and 0.59 for 140-7. Similarly, in descending order, the results of measurement of resist sensitivity (E_{th}) after development for 15 min were 811 mJ/cm^2 for 110-7, 929 mJ/cm^2 for 110-9, 932 mJ/cm^2 for 125-5, 938 mJ/cm^2 for 125-7, and 985 mJ/cm^2 for 125-9, 1595 mJ/cm^2 for 140-5, and 4658 mJ/cm^2 for 140-7. Thus, 125-7 yielded the highest development contrast, and 140-5, 140-7 yielded the lowest sensitivity.

4. Discussion

4.1 Relationship between development contrast and pattern profile

The patterning results indicate that the pre-baking condition of 125-7 affords the steepest sidewalls and least thickness decrease near the resist surface. The films prepared under conditions of 125-9, 110-9, 110-7, 125-5, 140-5 and 140-7 follow.

Table 2. shows a comparison of discrimination curves ($\tan\theta$) for the various pre-baking conditions. The 125-7 gives the highest value, followed by 125-9, 110-9, 110-7, 125-5, 140-5 and 140-7. This result suggests that enhanced development contrast is the reason for the high resolution and high rectangularity of 125-7.

The results of SOLID-C simulation using this discrimination data $R(E)$, where R denotes the average development rate and E denotes the exposure dose, are shown in Fig. 2. The simulation results also indicate that 125-7 produces the highest rectangularity, followed by 125-9, 110-9, 110-7, 125-5, 140-5 and 140-7. Thus, the

development contrast data supports the relationship between the various pre-baking conditions and the resulting resolution and rectangularity.

A SEM observation result corresponded to the simulation result well from pre-baking temperature 110 to 140 . On the other hand, a SEM observation result didn't correspond to the simulation result from pre-baking temperature 80 to 95 . This can be examined when it is because simulation software does not cope with the foaming phenomenon of N2.

4.2 N₂ bubbling model based on residual solvent

The question then arises as to the mechanism responsible for the decrease in resolution and rectangularity in the order 125-7, 125-9, 110-9, 110-7, 125-5, 140-5 and 140-7. This is first investigated based on the activation energies involved in pre-baking. Table 3. shows the development reaction rate constants for the various pre-baking conditions at exposure doses of 50, 500 and 2000 mJ/cm². Fig. 3 shows activation energies obtained from an arrhenius plot of the development reaction rate constants. The activation energy and frequency factor were estimated from the slope of the arrhenius plot of the development rate k_d (nm/s) and the pre-bake temperature [10] using the following equation.

$$\frac{d \ln k_d}{dT} = \frac{E}{RT^2} \quad (1)$$

where E denotes the activation energy (kcal/mol), T is the pre-bake temperature (Kelvin) and R is the gas constant (8.31442JK⁻¹mol⁻¹). At the 2000 mJ/cm² exposure dose, the activation energy were 7.47 (kcal/mol) for 80-5 to 95-5, -11.06 (kcal/mol) for 110-5 to 140-5. At the 500 mJ/cm² exposure dose, the activation energy were 4.71 (kcal/mol) for 80-5 to 95-5, -3.89 (kcal/mol) for 110-5 to 140-5. The activation energies were plus between 80 and 95 °C, and minus between 110 and 140 °C. The resist development process exhibits very different reactivity in these two regions. For exposure doses of 50 mJ/cm², the development rate increases linearly and the activation energies were minus value with falling temperature from 140 to 80 °C.

At the 2000 mJ/cm² exposure dose, the same tendency was seen for pre-baking conditions 140-7, 125-7, 110-7, 95-7, 80-7, 140-9, 125-9, 110-9, 95-9 and 80-9. For exposure doses of 50 and 500 mJ/cm², the development rate increases linearly and the activation energies were minus value with falling temperature from 140 to 80 °C. These phenomena demonstrate that the resist film condition can be categorized into two ranges of pre-baking temperature; between 80 and 95 °C , and between 110 and 140 °C.

Fig. 4 shows the transmission of the resist film before and after exposure, measured using the transmission measurement system. The transmission for the measurement wavelength of 420 nm were: approximately 11 % for pre-baking condition 80-5, approximately 11% for 95-5, approximately 0% for 110-5, approximately 0% for 125-5 and approximately 0% for 140-5. For pre-baking conditions 80-5 and 95-5, the transmission was approximately 11%, whereas the transmission was approximately 0% for 110-5, 125-5, and

140-5. This shows that the resist film condition is completely different in the two ranges of pre-baking temperature described above. The same tendency was seen for pre-baking conditions 80-7, 95-7, 110-7, 125-7, 140-7, 80-9, 95-9, 110-9, 125-9 and 140-9. Fig. 4(f) shows the measured transmission of the resist solvent, propyleneglycol monomethylether acetate (PGMEA). The transmission of PGMEA was 97 % for the measurement wavelength of 420 nm. Between 80 and 95 °C, the evaporation of PGMEA solvent is low and a large amount of residual solvent remains, increasing the transmission of the solvent for the measurement wavelength of 340 to 420 nm, thus increasing the transmission of the resist film to approximately 11%. The attenuated transmission for all wavelengths after exposure is due to cloudiness on the resist surface caused by N₂ bubbles from the resist [4]. In contrast, between 110 and 140 °C, a significant amount of PGMEA solvent evaporates, and there is little residual solvent, increasing the relative concentration of the PAC in the resist and reducing the transmission of the resist film to approximately 0 % for the measurement wavelength of approximately 340 to 420 nm. The measurement results for activation energy and transmission reveal that the amount of residual PGMEA solvent in the resist film differs between the two pre-baking conditions of 80 to 95 °C and 110 to 140 °C.

The amount of residual solvent in the resist film after pre-baking can then be examined to develop a bubbling model for N₂ generated in the resist film during exposure. The solvent evaporates off the resist surface during pre-baking, and the amount of evaporation depends on the pre-baking temperature and baking time. When the back of the substrate is baked by proximity baking, the solvent evaporates off the resist top surface, and as such the concentration of the residual solvent is expected to be higher near the top surface of the resist. Fig. 5 shows the amount of residual solvent after pre-baking, as measured by GC-MS. The amount of residual solvent in the resist film was as follows: 200 (µm/mg) for pre-baking condition 80-7, 160 (µm/mg) for 95-7, 120 (µm/mg) for 110-7, 86 (µm/mg) for 125-7, and 56 (µm/mg) for 140-7, demonstrating that the amount of residual solvent in the resist film is larger for lower baking temperature. Fig. 6 FT-IR spectrum data during pre-baking at 110 °C and Fig.7 shows the changes in the amount of PGMEA solvent during pre-baking, as measured using the PAGA-100. The peak at 1736 cm⁻¹, which indicates the amount of PGMEA, was measured during baking at each baking temperature. The amount of solvent changes sharply during the first 5 min of baking, changing only marginally after that.

The proposed N₂ bubbling model based on these results is shown in Fig. 8. The concentration of the residual solvent is higher near the resist surface, and a large amount of residual solvent remains at low baking temperatures between 80 and 95 °C. The N₂ generated during exposure is trapped in the residual solvent, preventing effective release of the N₂. The trapped N₂ is then released from the resist film as bubbling during development, which breaks the resist pattern profile and causes the pattern to peel away. At baking temperatures of 110 to 140 °C, where the amount of residual solvent is small, the N₂ generated by exposure is not trapped in the solvent, instead being released from the resist film. This results in very little or no N₂ bubbling during

development, improving patterning performance.

4.3 Change in the amount of photo active compound (PAC) in resist film

Fig. 9 shows the measurement results for the 2143 cm^{-1} peak due to azo coupling of the PAC for various varying baking times and temperatures, as determined using the PAGA-100. For baking temperatures of 80 to 110 °C, the change in azo coupling was small during baking. For 125 °C, the change in azo coupling was small for the first 10 min, then noticeably decreased, demonstrating that the PAC was decomposing. In this patterning experiment, baking was conducted for a maximum of 9 min. Within this time range, there was almost no decrease in azo coupling at baking temperature of 80 to 125 °C, suggesting that no PAC was decomposed due to baking heat at these temperatures. In contrast, at 140 °C, azo coupling absorption decreased sharply immediately after baking started, decreasing by 50 % after 5 min, 60 % after 7 min, and 70 % after 9 min, showing that the PAC was decomposing due to baking heat. The significant degradation of the sensitivity and resist profile at the baking temperature of 140 °C is therefore attributed to the reduced sensitivity due to the decrease in the amount of PAC, weakening the development retarding effect on unexposed sections of the resist.

4.4 Benard cell generation

Fig. 10 shows optical micrograph of the surface of the residual resist film after development for pre-baking conditions 80-7, 95-7, 110-7, 125-7 and 140-7. The temperature difference between the hot part near the baking plate and the cold surface of the resist during pre-baking generates marangoni convection, resulting in benard cells on the resist surface. The marangoni number is obtained by the following equation [11].

$$\text{Marangoni number} = \frac{(-d\delta/dT)\beta d^2}{\eta k} \quad (2)$$

where η is viscosity (g/cm·s), k is heat transfer constant (cm^2/sec), d is film thickness (cm), δ is surface tension (dyne/cm) and β is the temperature difference between the hot and cold parts (°C). This equation shows that with decreasing resist viscosity η , marangoni convection occurs more easily. When the pre-baking temperature is low, there is a large amount of solvent in the resist film, decreasing the resist viscosity, thus resulting in a large marangoni number. When the pre-baking temperature is high, there is only a small amount of solvent in the resist film, increasing the resist viscosity, thus resulting in a small marangoni number. According to the microscope observations, the marangoni number is large at low baking temperatures of 80 to 95 °C, resulting in many benard cells, whereas the marangoni number is small at high baking temperatures of 110 to 140 °C, generating few benard cells.

5. Conclusions

The resolution and rectangularity of thick-film resist were investigated experimentally for various pre-baking conditions. The results indicate that pre-baking condition 125-7 affords resists with the highest resolution and rectangularity, followed by 125-9, 110-9, 110-7 and 125-5. For 140-5 and 140-7 thickness loss at the top was significant, which degraded the resolution. For 80-7, 80-9, and 95-9 the pattern was broken and peeled due to N₂ bubbling, and for 80-5, 95-5, 95-7 and 140-9 adequate separation resolution was not obtained. The underlying mechanisms were considered by comparing the development activation energies for the different pre-baking conditions, by comparing the changes in the amount of solvent and PAC during pre-baking, by comparing the amount of residual solvent in the resist and the resist transmission after pre-baking, by observing Benard cells, and by conducting resist pattern simulations. A N₂ bubbling model was proposed, in which the N₂ generated in the resist film during the exposure process is considered to be trapped in the residual solvent in the resist film, governed by the amount of residual solvent and the compactness of the resist film. From the N₂ bubbling model and activation energy values for each pre-baking condition, it was determined that N₂ bubbling can be prevented by adopting pre-baking conditions that leave the smallest amount of residual solvent in the resist, afford a minus activation energy, and do not decompose the PAC. Thus, in the present work, as an approach to increasing the resolution that can be achieved with thick-film resist, it was confirmed that prevention of N₂ bubbling is important in minimizing pattern profile degradation, as is prevention of PAC decomposition. Having identified these major factors associated with pre-baking, future study will focus on optimal pre-baking methods and conditions based on these considerations.

6. Acknowledgements

The authors would like to thank Mr. Koji Saito, Mr. Kouichi Misumi of Tokyo Ohka Kogyo for providing resist materials and precious advice and Mr. Jeffrey Lane of QUINTEL for providing us with the UL7000 mask aligner system.

References

- [1] R. Arai, "Exposure machine for the magnetic head," *Electric Parts and Materials*, pp. 84-89, Feb. 2000.
- [2] Y. Shibayama, and M. Saito, "Influence of Water on Photochemical Reaction of Positive-Type Photoresist," *J. Appl. Phys.*, vol.29, pp. 2152-2155, Oct. 1990.
- [3] Y. Sensu, A. Sekiguchi, and Y. Miyake, : "Improved Resolution of Thick Film Resist (Effect of Development Technique)", *Advances in Resist Technology and Processing, Proc. SPIE*, vol. 4690, pp. 861-882, Mar. 2002.

- [4] Y. Senu, A. Sekiguchi, and Y. Miyake, : “ Study on Improved Resolution of Thick Film Resist (Verification by Simulation) ”, Advances in Resist Technology and Processing, Proc. SPIE, vol. 4345, pp. 921-935, Feb. 2001.
- [5] A. Sekiguchi, C. A. Mack, Y. Minami, and T. Matsuzawa, " Resist Metrology for Lithography Simulation, Part 2 : Development Parameter Measurements, " Proc. SPIE, vol. 2725, p. 49, Mar. 1996.
- [6] Erddmann A, Henderson C. L, Willson C. G, Henke W, " Influence of optical nonlinearities of photoresists on the photolithographic process : Applications, " Proc. SPIE, vol.3048, Mar. 1997.
- [7] Y. minami, A. Sekiguchi, " Defocus Simulation Using Observed Dissolution Rate in Photolithography. " Electronics and Communications in Japan, Part 2, vol.76, No. 11, 1993.
- [8] A. Sekiguchi, Y. Miyake and M. Isono, " Analysis of Deprotection Reaction in Chemically Amplified Resists Using an Fourier Transform Infrared Spectrometer with an Exposure Tool, " Jpn. J. Appl. Phys. vol. 39(2000), pp. 1392-1398, part 1, No. 3A, Mar. 2000.
- [9] T. Kokubo, " History of Research and Development for Positive Photoresist," Fuji Film Research and Development, No. 34, pp. 621-31, 1989.
- [10] M. Ono, S. Hasegawa, S. Yagi, " Detail Explanation of the Practice of Physical Chemistry, " pp. 278-307, Kyoritsu Shuppan Co. , LTD., Tokyo Japan, 1967.
- [11] Pearson. J. R. A., J. Fluid Mech., 19, 341, 1964.

Table 1. Lists the pre-baking conditions.

Bake Time (min)	5	7	9
Bake Temp. (°C)			
80	80-5	80-7	80-9
95	95-5	95-7	95-9
110	110-5	110-7	110-9
125	125-5	125-7	125-9
140	140-5	140-7	140-9

Table 2. Development contrast ($\tan\theta$), resist sensitivity (E_{th}) and E_{op} for the different Bake conditions.

Bake Condition	$\tan\theta$	E_{th} (mJ/cm ²)	E_{op} of Simulation (mJ/cm ²)	Patterning Expo. dose (mJ/cm ²)
80-5	0.9	756	760	500
80-7	1.0	654	640	500
80-9	0.8	625	570	500
95-5	1.1	624	610	600
95-7	1.1	670	640	600
95-9	0.9	705	660	600
110-5	2.4	691	700	820
110-7	3.6	811	820	900
110-9	3.7	929	935	960
125-5	3.5	932	920	950
125-7	4.3	938	1010	1050
125-9	4.1	985	1040	1170
140-5	3.3	1595	1500	2250
140-7	0.6	4658	4000	4780
140-9	2.0	5192	5200	6000

Table 3. The energy of activation for the different Bake conditions.

(a) bake time 5 min, (b) bake time 7 min, (c) bake time 9 min.

(a) Bake Time 5 min				(Kcal / mol)
Exposure dose (mJ/cm²)	50	500	2000	
Bake Temp. (°C)				
80 to 110	-0.4134	4.711	7.472	
125 to 140	-0.4134	-3.896	-11.061	

(b) Bake Time 7 min				(Kcal / mol)
Exposure dose (mJ/cm²)	50	500	2000	
Bake Temp. (°C)				
80 to 110	-1.926	-2.039	4.806	
125 to 140	-1.926	-2.039	-11.251	

(c) Bake Time 9 min				(Kcal / mol)
Exposure dose (mJ/cm²)	50	500	2000	
Bake Temp. (°C)				
80 to 110	-2.076	-4.072	0.5611	
125 to 140	-2.076	-4.072	-12.23	

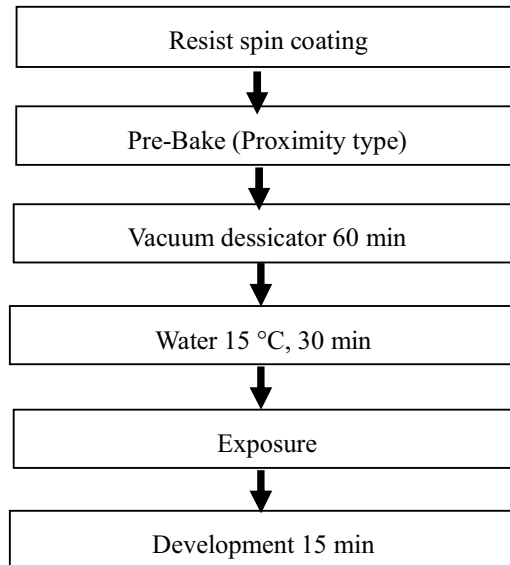
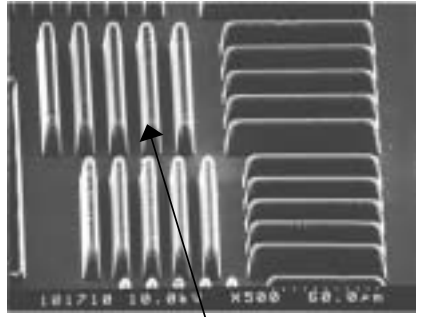
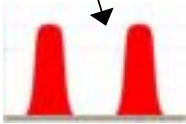
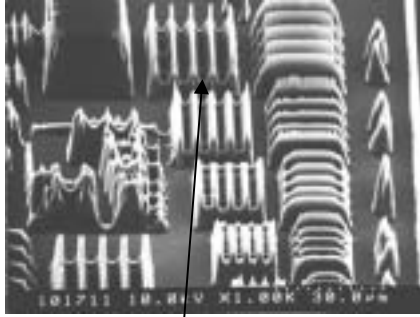
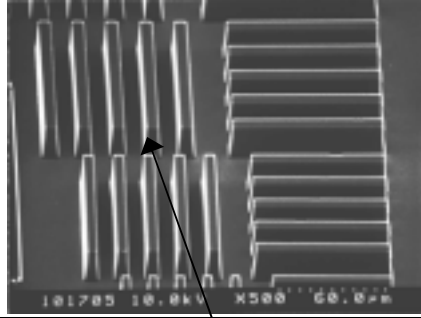
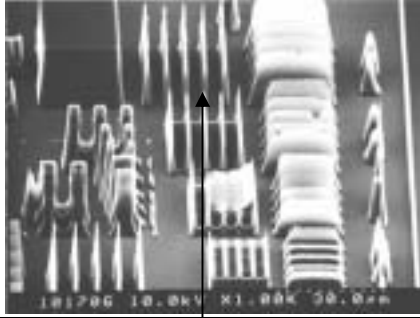
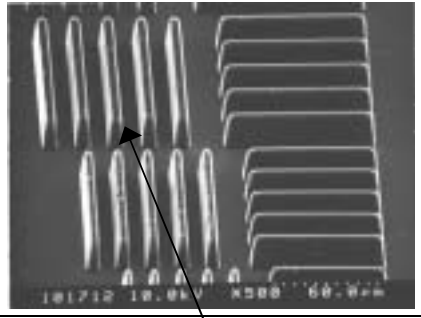
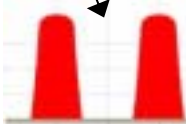
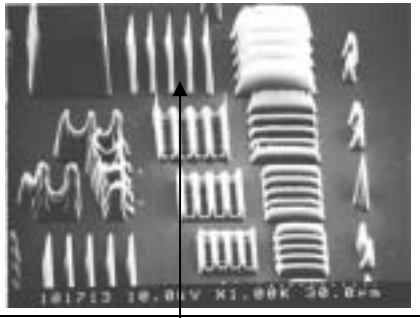
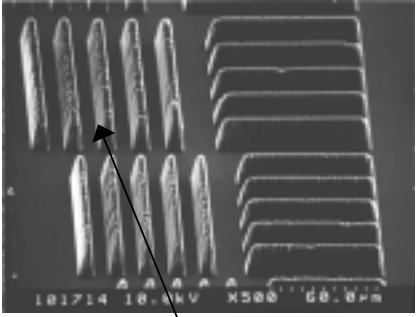
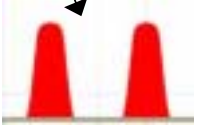
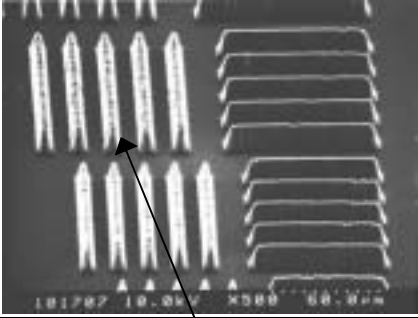
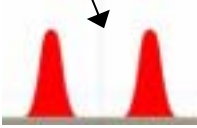
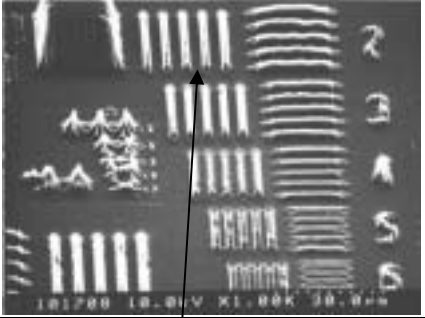
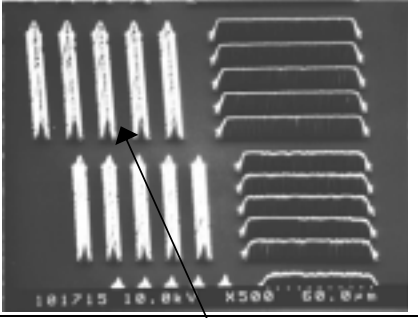
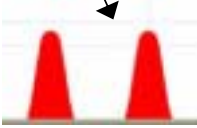


Fig. 1. Sample preparation process flow.

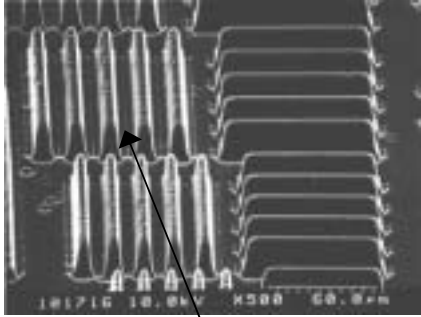
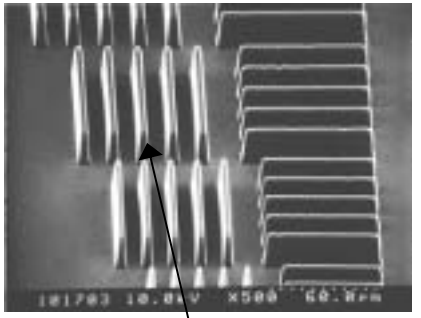
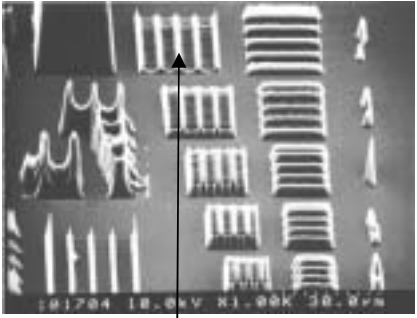
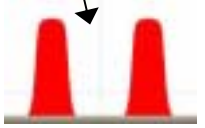
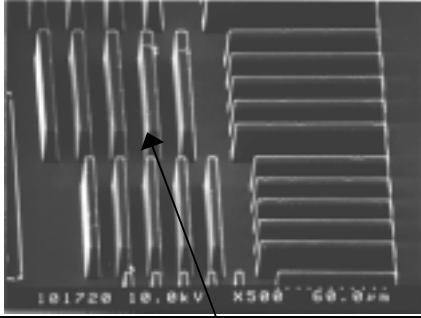
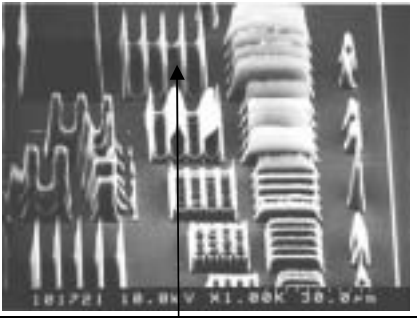
(a) Beke Temp. 125 °C

Bake Time (min)	10.0 μ m L/S	2.8 μ m L/S
5	 	 
7	 	 
9	 	 

(b) Beke Temp. 140 °C

Bake Time (min)	10.0 μm L/S	2.8 μm L/S
5	 	
7	 	 
9	 	

(c) Beke Temp. 110 °C

Bake Time (min)	10.0 μm L/S	2.8 μm L/S
5		
		
7		
		
9		
		

(d) Beke Temp. 95 and 80 °C

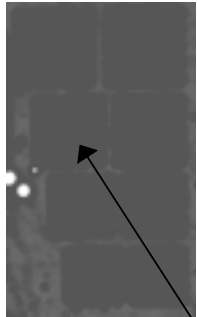
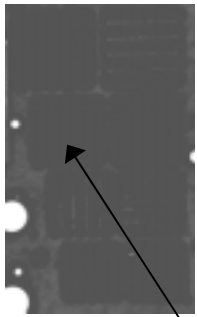
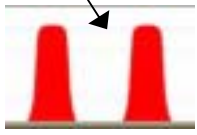
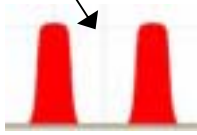
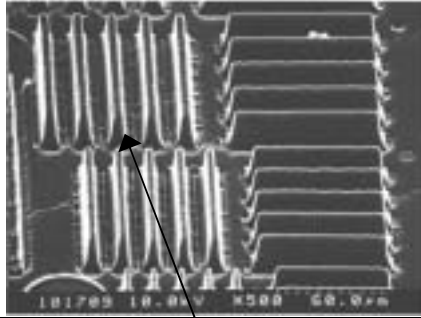
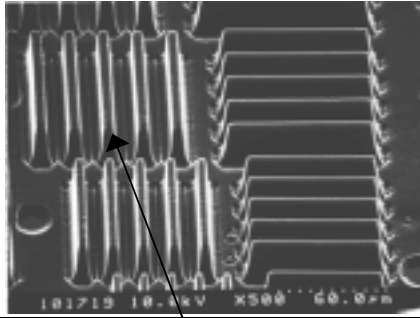
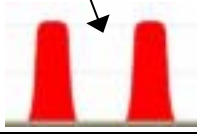
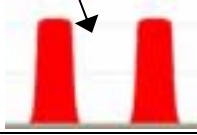
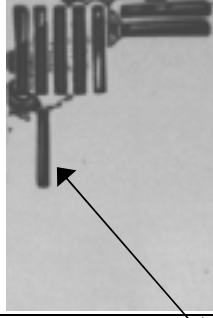
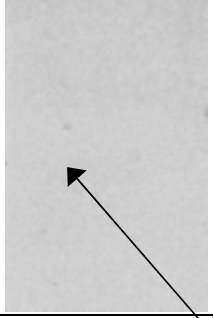
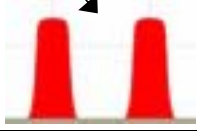
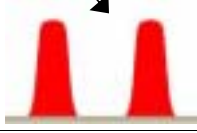
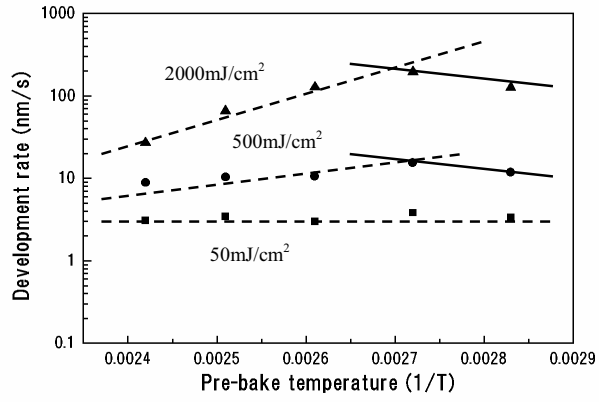
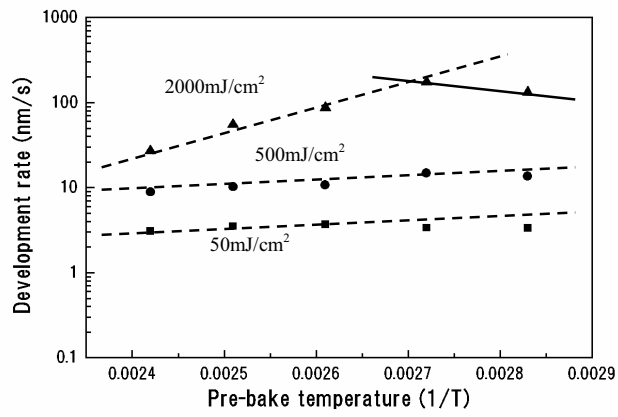
Bake Time (min)	Temp. 95 °C, 10.0 μm L/S	Temp. 80 °C, 10.0 μm L/S
5		
		
7		
		
9		
		

Fig. 2. SEM, optical micrograph and simulation data of the resist patterns.

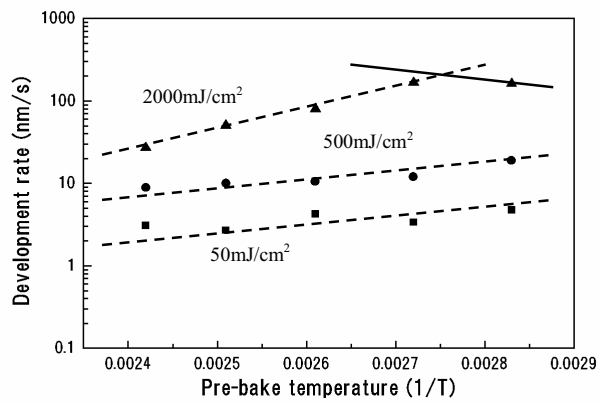
(a) bake temp. 125 °C, (b) bake temp. 140 °C, (c) bake temp. 110 °C, (d) bake temp. 95 and 80 °C.



(a)

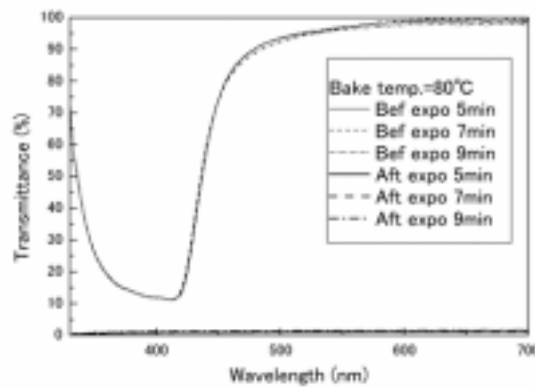


(b)

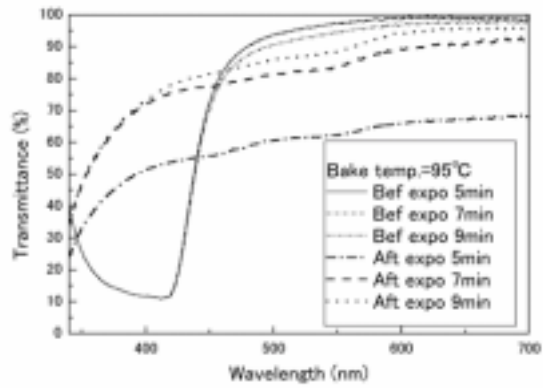


(c)

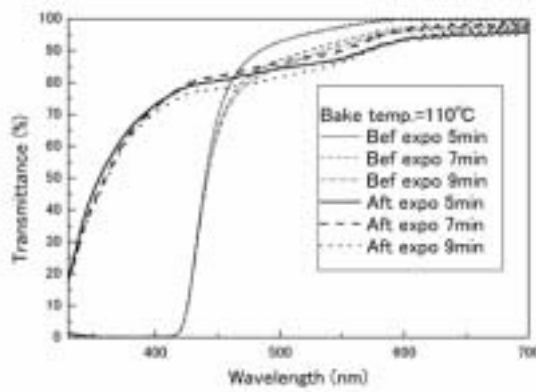
Fig. 3. Arrhenius plot at (a) bake time 5 min, (b) bake time 7 min and (c) bake time 9 min.



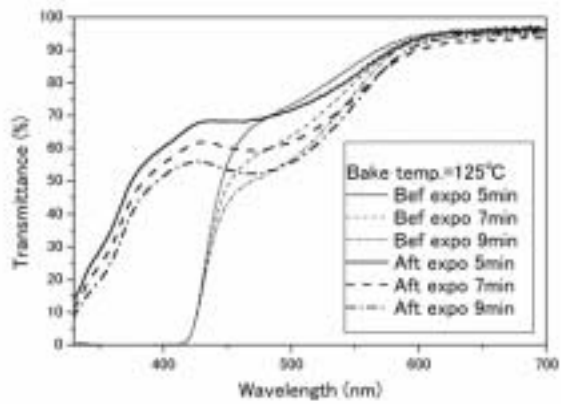
(a)



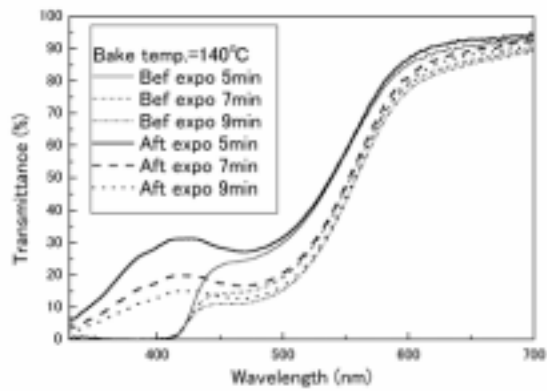
(b)



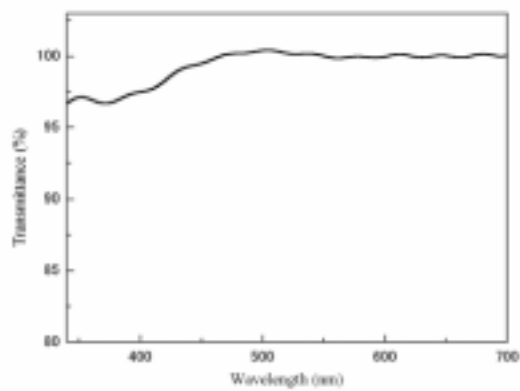
(c)



(d)



(e)



(f)

Fig. 4. The transmittance of the resist film before and after exposure.
 (a) bake temperature 80 °C, (b) bake temperature 95 °C, (c) bake temperature 125 °C,
 (d) bake temperature 125 °C, (e) bake temperature 140 °C and (f) PGMEA.

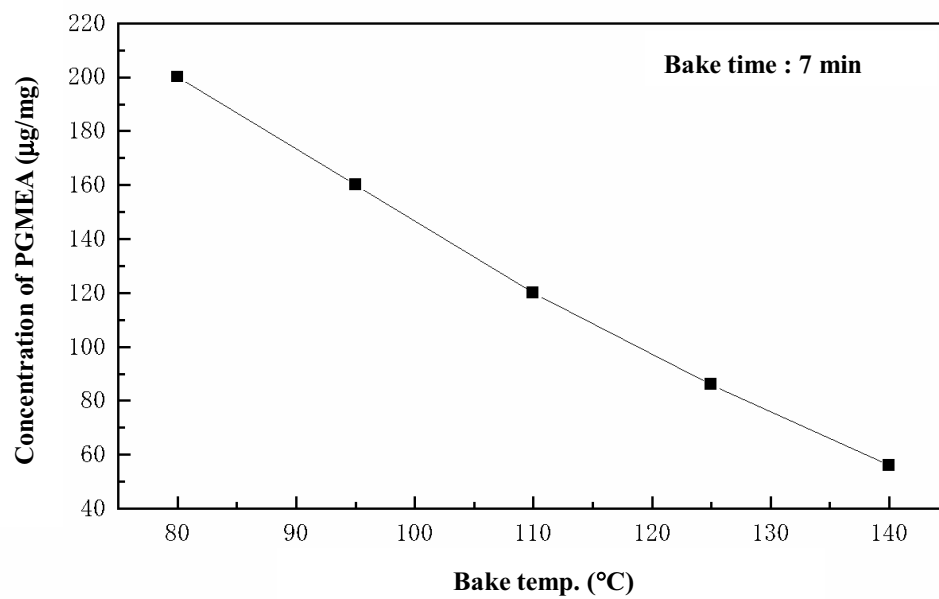


Fig. 5. The amount of residual solvent after pre-baking.

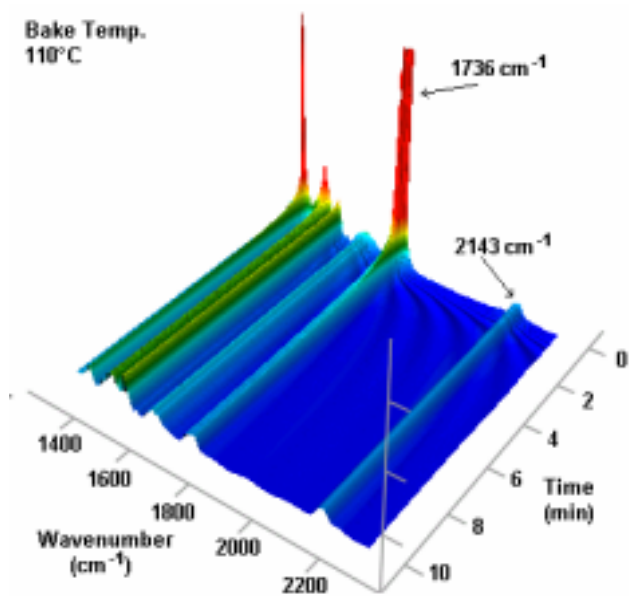


Fig. 6. The FT-IR spectrum data during pre-baking at 110 °C.

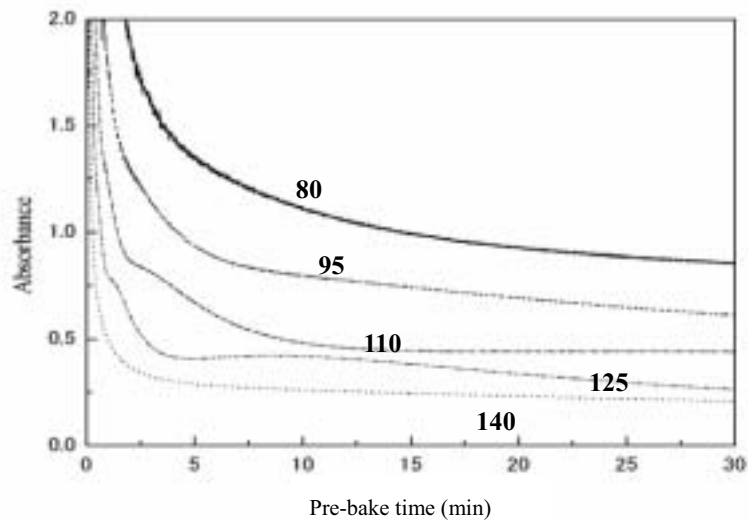


Fig. 7. Relationship between absorbance and pre-bake time for carbonic-bond absorption at 1736cm^{-1} .

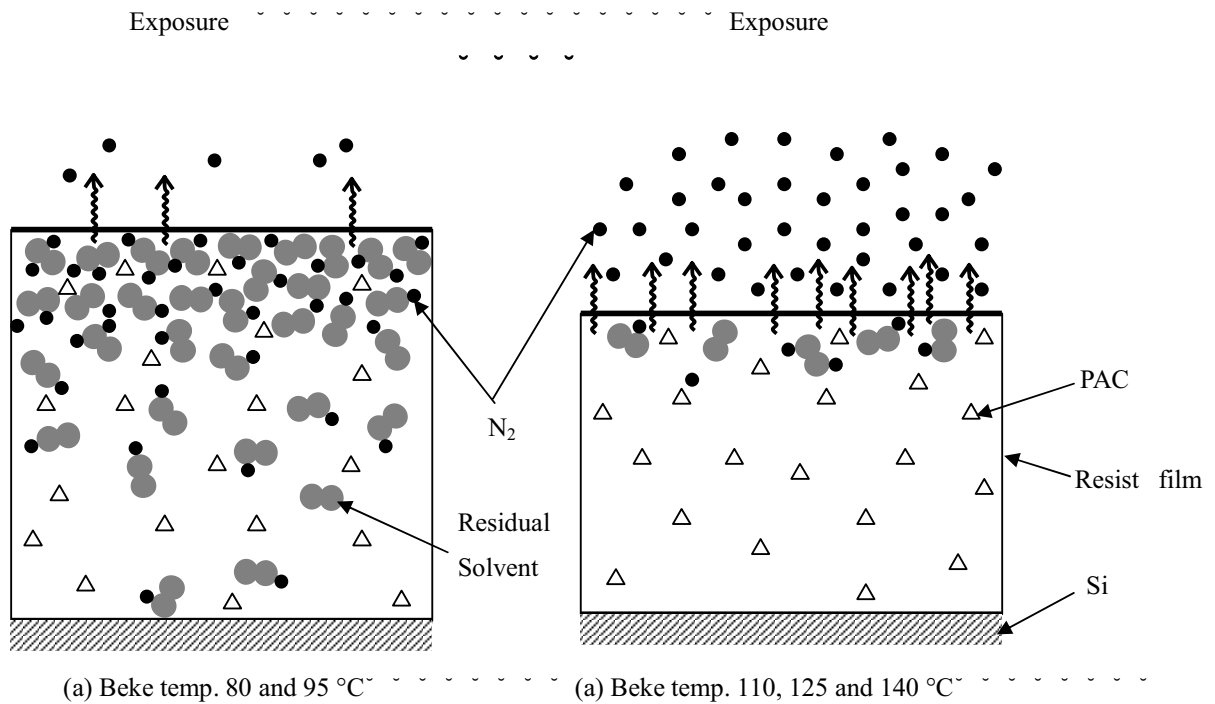


Fig. 8. N_2 bubbling model.

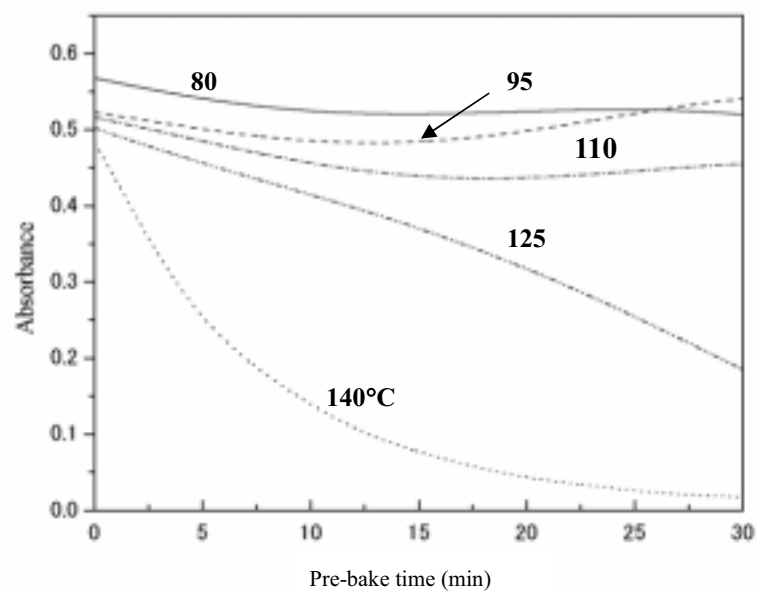
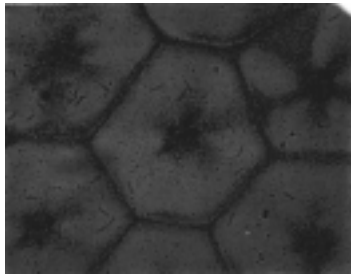
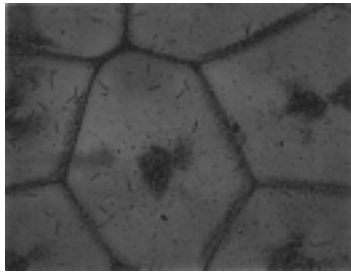


Fig. 9. Relationship between absorbance and pre-bake time for azo-bond absorption at 2143cm^{-1} .

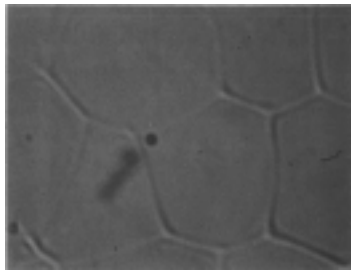


Bake conditions

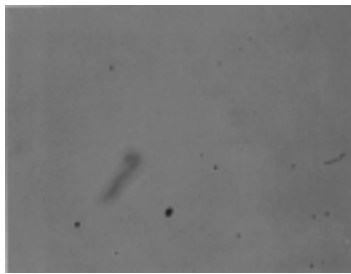
80-7~ (Temp. : 80 °C, Time : 7 min)



95-7~ (Temp. : 95 °C, Time : 7 min)



110-7 (Temp. : 110 °C, Time : 7 min)



125-7~ (Temp. : 125 °C, Time : 7 min)



140-7~ (Temp. : 140 °C, Time : 7 min)

Fig. 10. Micrograph of the surface of the residual resist film after development.